

## 2 Determination of the selection function and related material properties

---

### Abstract

*The particle size distribution of pharmaceutically active materials and other fine chemicals determines the performance of the final product to a large extent. Often milling of these particles is necessary. It is not possible to determine the milling conditions only on the basis of the particle size distribution of the starting material, because the (mechanical) properties of the material determine the desired milling conditions too. It is often not possible to optimize milling conditions experimentally because the material is scarcely available. A theoretical approach towards predicting the best milling conditions is needed. The purpose of this study was to develop a method to predict the desired milling conditions given a specific (organic) solid material. The selection function and the breakage distribution function are usually the starting point in modeling the milling process. The selection function is the parameter that includes the material and mill properties. Dimensional analysis made it possible to correlate the selection function with material properties. A set of theories available in the literature enables prediction of the material properties. For different compounds (lactose, paracetamol, a steroidal compound, and two heterocyclic compounds) the selection functions were calculated. The calculations predict differences: lactose reduces slowly in size, while one of the heterocyclic compounds shows the most intense fracture.*

---

Part. Part. Syst. & Charact. 22 (2002) 133-140

## **2.1 Introduction**

Jet milling is a well established technique for grinding material. The milling behaviour of a material and therefore the resulting particle size distribution is governed by the mechanical properties of the material, its initial particle size distribution and the milling conditions. The influence of material properties on grinding behaviour is widely recognized (e.g. 1). However, controlling the grinding process on the basis of material properties is less established. At this moment there is no method that allows prediction of the grinding behaviour of particles based on material properties (1). This lack of information leads to the disappointing experience that each milling test with a new or unknown powder has to start from the beginning. This consumes a lot of effort and material. Due to the fact that knowledge of material properties is crucial for choosing the proper operating conditions, the aim of this study was to develop a model which incorporates material properties to predict the drug substance particle size distribution after milling a priori. The proposed model incorporates mechanical material properties as well as process conditions. As most of the time, the required material properties are unknown, special emphasis was placed on the theoretical and experimental determinations.

## **2.2 Theoretical approach**

### **2.2.1 Selection Function and Breakage Distribution Function**

The basis in modeling the grinding process is usually the selection function and the breakage distribution function (2). The selection function is the probability of a particle of size  $i$  to break in a unit of time. The breakage distribution function describes the size distribution after breakage of a particle of a given size. Knowledge of both functions allows the calculation of the change in the particle size distribution with grinding time. Berthiaux (3) demonstrated that it is possible to derive the breakage distribution function from the selection function.

Therefore, our attention is focused on the determination of the selection function. A method has been developed to calculate the selection function based on dimensional analysis and on fracture mechanics.

### **2.2.2 Prediction of selection function**

Peukert indicated that the total selection function consists of two parts, representing the process (the “mill function”) and the material parameters (the “material function”) (1, 4). The mill function represents the type of mill and processing conditions, e.g. grinding pressure which affects the energy density. For validation of the model one specific type of mill will be used. So, most of the parameters of the mill function have constant values. In the current study, only the grinding pressure has been varied. The reason for this is that the intention was to focus on mechanical material properties. For this specific situation the only equipment related variable is milling pressure, which affects the kinetic energy, and the energy density supplied to the mill. This means that the selection function consists of a kinetic energy density term (see Table 2-1 for a list of all parameters included in the dimension analysis).

A body under strain stores strain energy. This elastic strain energy is the energy input up to the moment of particle fracture (5). The total energy per unit fracture area, which must be produced as the crack propagates, is called the fracture energy. Griffith (6) demonstrated that the crack propagation stress is inversely proportional to the square root of the flaw size. It has been observed by several authors (6,7) that the presence of initial flaws determines the fracture pattern in particles. When a crack propagates it tends to branch. With an energy model Weichert (7) derived that the crack pattern is very consistent, i.e. equal for all particles. All dimensions of the crack pattern are proportional with the ratio of the initial flaw size to particle size. In addition, in the modeling of particle impact breakage, Potapov and Campbell (8) made the crack length dimensionless by dividing by the particle size. The same correlation

was suggested by Rumpf (9), who stated that the crack pattern can be described by one characteristic length, so that the same fracture pattern is determined by a dimensionless value which is a constant. Using dimensional analysis and a fracture mechanic model Rumpf (9) described the similarity of breakage of particles of similar shape but different materials. The result was that the following parameters appear to affect the fracture behaviour of particles: energy density per unit mass of material, the crack propagation velocity, the velocity of propagation of elastic waves, the deformation velocity, and the ratio of the initial flaw length to the initial particle size. Assuming a constant mill load this implies that energy input per unit of mass is proportional with kinetic energy density. Vogel and Peukert (4) stated that values of the fracture velocity, velocity of elastic waves, and deformation velocity are in the same order of magnitude. This makes it possible to combine these parameters and to include only the fracture velocity in the dimensional analysis. Following the approach of Marsh (10) the terminal fracture velocity is the square root of the ratio of the yield pressure to the particle density. Modeling efforts from Ghadiri (11) and Taylor et al. (12) indicated that additional relevant parameters are the particle density, the impact velocity, the stress intensity factor, and a constraint factor given by the ratio of the hardness to the yield pressure. Finally, on the basis of the work from Schönert (13), the decision was not to include surface energy in the model since the fracture energy is considerably larger than the surface energy. From this evaluation it follows that the selection function must consist of parameters indicated in Table 2-1.

Table 2-1 Origin of parameters in dimensional analysis.

Parameter	Source	Described by	Source
Fracture energy	(5)	$E_{frac}$	(5)
Crack propagation stress	(6)	$\left(\frac{1}{x_i}\right)^{0.5}$	(6)
Size of initial flaws	(6,7,9)	$\frac{l}{x_i}$	(6,7,9)
Kinetic energy density (per unit of mass)	(9)	$\frac{E_{kin}}{V}$	This chapter
Crack propagation velocity	(9)	$\frac{P_y}{\rho}$	(4,10,11)
Velocity of elastic waves	(9)	$\rho$	
Deformation velocity	(9)		
Density	(11)		
Stress intensity factor	(11)	$K_{1C}$	(11)
Hardness	(11)	$H$	(11)
Surface energy	(13)	Not included	(13)

*Explanation: The first two columns give the relevant parameters together with the source reference. The third column gives the actual symbol that describes the parameter. The fourth column provides the source(s) that correlate the symbol in the third column with the parameters indicated in the first column.*

To determine the selection function, dimensional analysis has been performed (appendix 1) with these parameters and resulted in:

$$S_i = c \frac{E_{kin} E_{fract} \sqrt{\frac{P_y}{\rho}}}{V H \sqrt{x_i} K_{1C}} \left(\frac{\ell}{x_i}\right) \quad (1)$$

The check on the validity of the model is shown, for reasons of readability, in chapter 3 (14). Eq. (1) requires quantifications of mechanical properties. Often these mechanical properties are unknown and need to be determined or at least estimated. The next chapter describes the methods which are used to determine these mechanical material properties.

### 2.2.3 Methods to determine mechanical material properties

For a variety of solids it has been shown that there is a relationship between the mechanical properties of organic crystals and their molecular properties. An example is the relation with the solubility parameter (14). The solubility parameter of a material is a thermodynamic parameter that represents the amount of energy which is necessary to remove a molecule from the lattice in which it is placed. Hence, it is a direct measure of the attraction that atoms or molecules have for one another. It is possible to quantify the solubility parameter of a material in a number of ways. A common approach is to use the group contribution method like the Hanssen (16) approach. It appeared that there is a relation between the stress intensity factor  $K_{IC}$  and the solubility parameter (17):

$$K_{IC} = 0.00026 \delta^2 \quad (2)$$

For determination of the material strength the decision was to use the tensile strength for which it is possible to correlate it with the solubility parameter (17):

$$\sigma_o = 0.0183 \delta^2 \quad (3)$$

Roberts and Rowe (17) correlated the tensile strength of a massive compact with the solubility parameter. The assumption in this paper is that this value corresponds with the highest attainable value of a single crystal.

The tensile strength of a particle depends on its size and Weibull statistics were used to calculate the tensile strength – particle volume relation (5,19):

$$\sigma = \sigma_0 \left( \frac{V_0}{V} \right)^{\frac{1}{m}} \quad (4)$$

Following the discussion by Vogel and Peukert the Weibull coefficient  $m$  is supposed to have a constant value of 4 (4).

The yield strength of the particles can be determined using a compaction experiment. A frequently applied relation (at least in pharmaceutical industry) is that proposed by Heckel (54). Heckel suggested to linearise the porosity-pressure relation of powders:

$$-\ln(\varepsilon) = K \cdot P_c + A \quad (5)$$

The linear part of the curve has slope  $K$  and this slope is related to the yield strength by:

$$\sigma_c = \frac{1}{3 \cdot K} \quad (6)$$

It is known that the yield pressure of a material is approximately equal to 3 times the yield strength hence the reciprocal of  $K$  can be regarded as numerically equal to the mean yield pressure (21):

$$P_y = 3 \cdot \sigma_c \quad (7)$$

The limitation of the method is that bulk mechanical properties are determined instead of single crystal properties. However, the yield pressure determined with this method shows good agreement with literature values obtained with indentation testing (21).

The next step is to determine the hardness of the material under investigation. There are a number of definitions of hardness, but in general the hardness can be defined as the resistance offered by a given material to external mechanical action endeavouring to scratch, indent or in any other way affect its surface (51). The hardness of materials can be estimated with the equation originally proposed by Tabor (23) and modified by Marsh (56):

$$\frac{H}{P_y} = 0.07 + 0.6 \cdot \ln \frac{Y}{P_y} \quad (8)$$

Following Roberts and Rowe (21) it is assumed that the ratio  $H$  over  $P_y$  has a value of 2.8, making that:

$$\frac{H}{P_y} = 2.8 \text{ and } \ln \frac{Y}{P_y} = 4.55 \quad (9 \text{ a,b})$$

Calculation of the kinetic energy  $E_{kin}$ , requires mill settings. The gas velocity in the jet can be calculated from the grinding pressure, the gas flow and internal diameter of the jets. For simplicity, the assumption is that the particle velocity (impact velocity) has the same value as the gas velocity has. Table 2-2 gives the calculated particle velocities at four different grinding pressures.



## 2.3 Experimental

Of five different model compounds the mechanical properties were determined: lactose monohydrate (DMV, Veghel, The Netherlands), paracetamol (BUFA, Uitgeest, The Netherlands), Org 12962 (a heterocyclic compound), Compound A (a heterocyclic compound), and Add-Neop (a steroid). The latter three materials were from Diosynth, Oss, The Netherlands.

The porosity-pressure relation of the model compounds was investigated using a high speed compression simulator (ESH, Brierley Hill, UK). This compression simulator enables the assessment of compaction behaviour with single tablets. A sample of 500 mg was compressed into a cylindrical compact with a diameter of 13 mm. Compression load and compact volume with time were recorded. The average punch speed was 3 mm/s. The compression profile was sinusoidal. The true densities of the drug substances have been determined with a gas pycnometer (AccuPyc 1330, Micromeritics) using nitrogen as test gas. The mill has a chamber volume of 2100 cm<sup>3</sup>, the internal diameter of the nozzles is 1.8 mm (this represents an Alpine fluidized bed opposed jet mill type 100AFG).

## 2.4 Results and discussion

The starting point was the calculation of the cohesive energy density on the basis of group contributions. With these values the stress intensity factor and particle tensile strength were calculated (Table 2-3). The crystal volume of paracetamol was taken from (24) and the crystal volumes of the other compounds can be found in reports from in-house development activities for the specific compounds. The unit crystal volume of add-neop is unknown and has been estimated by taking the average value of a number of steroids (since add-neop is an intermediate compound for the production of steroids).

Table 2-3 The cohesive energy density, the stress intensity, the true density, and the unit crystal volume of the five model compounds.

	$\delta$ [MPa <sup>1/2</sup> ]	$K_{Ic}$ [Pa.m <sup>1/2</sup> ]	$\rho$ [kg/m <sup>3</sup> ]	$V_o$ [m <sup>3</sup> ]
Add-Neop	20.2	$1.06 \cdot 10^5$	1159	$1.68 \cdot 10^{-27}$ *
Lactose	45	$5.3 \cdot 10^5$	1542	$7.76 \cdot 10^{-28}$ (25)
Paracetamol	26.1	$1.8 \cdot 10^5$	1292	$7.74 \cdot 10^{-28}$ (24)
Org 12962	25.7	$1.7 \cdot 10^5$	1602	$2.52 \cdot 10^{-27}$ **
Compound A	26.1	$1.8 \cdot 10^5$	1338	$1.12 \cdot 10^{-27}$ **

\* *Average value of a number of steroids from in-house determinations*

\*\* *In-house determinations*

Using solubility parameters for estimating of mechanical material properties has some limitations. It should be remembered that the theory of the solubility parameter is based on solution theory. Solids are approximated as liquids with large interaction. Crystallinity of the materials is not included. This means that specific interactions (such as hydrogen bonds) between molecules are not included.

Irregularities in shape of the material can greatly affect the size reduction process. Moreover, it is also not possible to take aspects like anisotropy into consideration. Because of these aspects the predictions of mechanical properties on the basis of solubility parameters are order-of-magnitude estimations (26,27). The error of the prediction is typically 20% (17).

Figure 2-1 shows the linearised porosity-pressure relation of lactose monohydrate as proposed by Heckel. The Heckel plots of the other model compounds are depicted in Appendix 2.

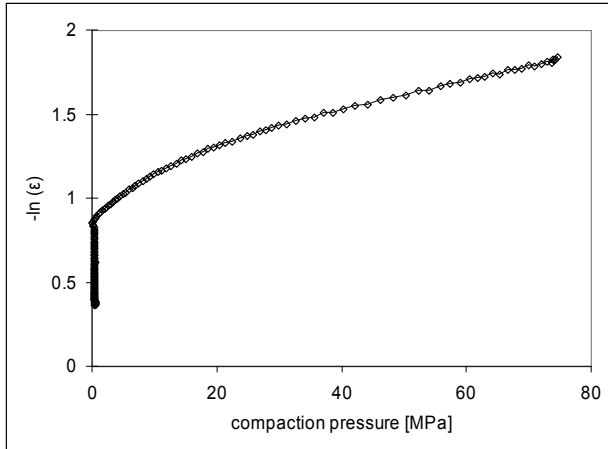


Figure 2-1 Heckel plot of  $\alpha$ -lactose monohydrate. Average punch speed during compaction was  $3 \text{ mm}\cdot\text{s}^{-1}$ .

Based on the data obtained from the Heckel plot and the equation of Marsh (56) values of yield strength, yield pressure and hardness were calculated (Table 2-4).

Table 2-4 Mechanical properties of the five model compounds as determined with the Heckel plot and equation of Marsh.

	$K$	$\sigma_o$ [MPa]	$\sigma_c$ [MPa]	$P_y$ [MPa]	$H$ [MPa]	$Y$ [GPa]
Add-Neop	0.0325	7.47	10.2	30.7	73.7	1.5
$\alpha$ -Lactose monohydrate	0.0097	29.1	33.3	103.0 (123 (28))*	288.4	9.7 (7.6(29))* (13.5(29))
Paracetamol	0.0139	13.95	23.9	74.7 (74 (28))*	172.1	3.5 (5.7(29))*
Org 12962	0.0587	12.09	5.7	17.0	40.8	0.82
Compound A	0.0139	12.46	23.9	71.6	200.6	6

\* *In brackets: values reported in literature.*

The experimentally determined yield pressures of lactose and paracetamol are in reasonable agreement with those reported by Doelker (28). The values of Young's modules of lactose and paracetamol coincide reasonably well with those reported by Roberts and Rowe (21). However, it must be mentioned that the reported value for the Young's modulus of paracetamol relates to direct compressible paracetamol whereas we used a different type of paracetamol.

The next step is to calculate the selection functions of the materials using the data in Tables 2-1, 2-3, and 2-4. However, since the constant value ( $c$ ) and the flaw length to particle size ratio ( $\ell/x_i$ ), which is also considered to be a constant, are not known, the selection function needs to be rearranged. The "reduced selection function" ( $S'_i$ ) has been defined, which only contains the variable parameters (the term denoted between the square brackets in eq (13)).

The selection function becomes:

$$S_i = c \left[ \frac{E_{kin} E_{fract} \sqrt{\frac{P_y}{\rho}}}{VH \sqrt{x_i} K_{lc}} \right] \left( \frac{\ell}{x_i} \right) = c S'_i \left( \frac{\ell}{x_i} \right) \quad (13)$$

Figure 2-2 shows the reduced selection functions as a function of particle size of the different materials.

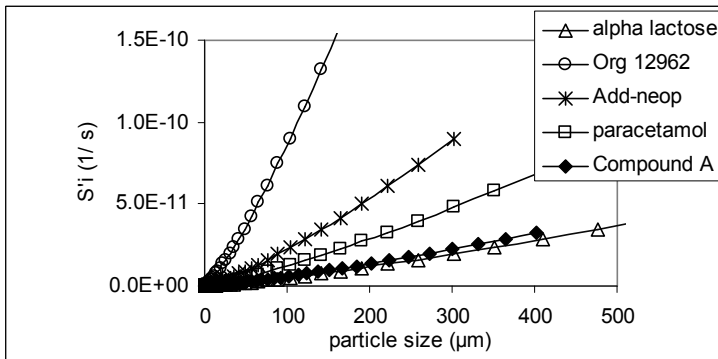


Figure 2-2 Predicted reduced selection functions of the model compounds. Simulated milling pressure is 5 bar.

Chapter 3 will describe the experimental validation of the model. There, the (constant) value  $(c \cdot \ell / x_i)$  will be determined.

The differences between the predicted rates of breakage for the different materials are obvious. Moreover, the difference in the rate of breakage for the different sizes is also clear. Smaller particles exhibit a smaller breakage probability compared with larger particles. The presented method describes the grinding kinetics allowing to make a distinction between different materials and the selection function can be calculated.

## 2.5 Conclusion

A method has been developed which predicts the selection function (particle rate of breakage function) for different materials. The method incorporates both mechanical material properties as well as a (limited) set of process conditions. The selection function depends on a number of parameters and a dimension analysis leads to:

$$S_i = c \frac{E_{kin} E_{fract} \sqrt{\frac{P_y}{\rho}}}{V H \sqrt{x_i} K_{1C}} \left( \frac{\ell}{x_i} \right) \quad (1)$$

The mechanical material properties are estimated using several methods and agree reasonably well with reported values available in literature. These material properties allow for a differentiation between various compounds. With the reported selection function the fraction of particles which are reduced in size during grinding can be determined for different materials.

## 2.6 Appendix 1: dimensional analysis

From the analysis (section 2.2.2) it appeared that the selection function  $S_i$  depends on the following physical properties:

$$S_i = f(E_{kin}, V, E_{fract}, x_i, \ell, P_y, \rho, K_{1C}, H) \quad (14)$$

Taking into account that  $E_{kin}/H \cdot V$  is dimensionless leads to:

$$S_i = f((E_{fract})^a \cdot (x_i)^b \cdot (\ell)^c \cdot (P_y)^d \cdot (\rho)^e \cdot (K_{1C})^f) \quad (15)$$

Filling in the basic dimensions (table 5) leads to:

$$(T): \quad -1 = -2 \cdot a - 2 \cdot d - 2 \cdot f \quad (16a)$$

$$(M): \quad 0 = a + d + e + f \quad (16b)$$

$$(L): \quad 0 = -a + b + c - d - 3 \cdot e - 0.5 \cdot f \quad (16c)$$

Table 2-5 Dimensions of parameters involved.

Dimension	$S_i$	$E_{kin}$	$E_{fract}$	$\rho$	$V$	$l$	$H$	$x_i$	$P_y$	$K_{ic}$
M	0	1	1	1	0	0	1	0	1	1
L	0	2	-1	-3	3	1	-1	1	-1	-0.5
T	-1	-2	-2	0	0	0	-2	0	-2	-2

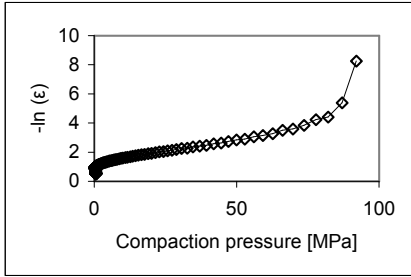
Dimensional analysis yields 3 equations with 6 unknown variables. Therefore, some assumptions are necessary. Based on the analysis described in chapter 2.2 it is assumed that  $b = -1.5$  [6,8],  $c = 1$  [8],  $d = 0.5$  [9] and,  $e = -0.5$  [9]. Finally, this leads to  $a = -1$  and  $f = -1$ , i.e.:

$$S_i = f((E_{kin})^1 (V)^{-1} (E_{fract})^1 (x_i)^{-1.5} (\ell)^1 (P_y)^{0.5} (\rho)^{-0.5} (K_{ic})^{-1} (H)^{-1}) \quad (17)$$

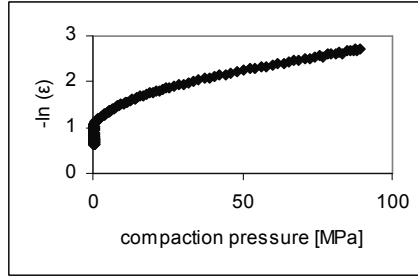
Hence:

$$S_i = c \frac{E_{kin} E_{fract} \sqrt{\frac{P_y}{\rho}}}{V H \sqrt{x_i} K_{ic}} \left( \frac{\ell}{x_i} \right) \quad (18)$$

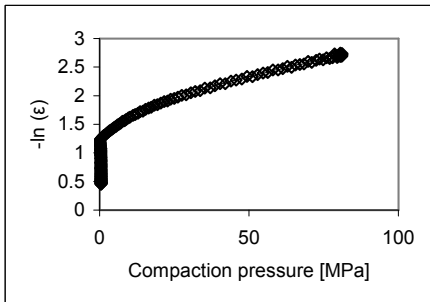
## 2.7 Appendix 2: Heckel plot of model compounds



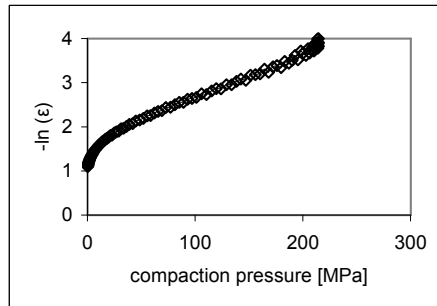
Heckel plot of Add Neop



Heckel plot of compound A



Heckel plot of Paracetamol



Heckel plot of Org 12962

Figure 2-3 Heckel plots of the model compounds. Average punch speed during compaction was  $3 \text{ mm}\cdot\text{s}^{-1}$ .



Table 2-2 Grinding pressure and corresponding velocity of grinding gas.

Grinding pressure [Bar]	Corresponding volume flow [m <sup>3</sup> /h]	Corresponding volume at S.T.P* [(normal)m <sup>3</sup> /h]	Gas velocity [m/s]
3.5	6.86	60	224
4	7.52	63	245
5	8.68	68	283
5.5	9.21	73	300

\* *Standard Temperature and Pressure.*

The mass of the particle is simply calculated from its size and density assuming spherical particles. Helium pycnometry is the method of choice to determine the material density.

The fracture energy is calculated using the approach of Yashima et al (5):

$$E_{fract} = 0.832 \left( \frac{1-\nu^2}{Y} \right)^{\frac{2}{3}} x_i^{\frac{1}{3}} P_c^{\frac{5}{3}} \quad (10)$$

When a sphere is compressed by the point loading method on two diametrically opposed points, the particle strength  $\sigma$  of the material is given by eq. 11 (5):

$$\sigma = \frac{2.8 P_c}{\pi x_i^2} \quad (11)$$

Combining eq. (10) and eq. (11) gives eq. (12) representing the energy required for fracture:

$$E_{fract} = 0.896 \left( \frac{1-\nu^2}{Y} \right)^{\frac{2}{3}} \sigma^{\frac{5}{3}} \pi^{2/3} \quad (12)$$

It is now easy to calculate the fracture energy when it is realized that poisson's ratio of many organic materials has a value of around 0.3 (18). This means that  $(1-\nu^2) \approx 1$ .

## 2.8 Appendix 3: Nomenclature

$A$	constant in the Heckel equation	[-]
$c$	Constant	[-]
$E_{fract}$	fracture energy	[J/m <sup>3</sup> ]
$E_{kin}$	kinetic energy of particles	[J]
$H$	hardness	[Pa]
$K$	constant in the Heckel equation	[Pa <sup>-1</sup> ]
$K_{IC}$	stress intensity factor	[Pa m <sup>1/2</sup> ]
$m$	Weibull's Coefficient of Uniformity	[-]
$P_c$	Compressive load	[N]
$P_y$	yield pressure	[Pa]
$\rho$	density	[kg/m <sup>3</sup> ]
$\sigma$	tensile strength	[Pa]
$\sigma_0$	strength of a particle of unit volume $V_0$	[Pa]
$\sigma_c$	yield strength	[Pa]
$S'_i$	modified selection function	[1/s]
$S_i$	particle breakage rate of a particle with size $i$ per time interval	[1/s]
$V$	volume of mill chamber	[m <sup>3</sup> ]
$V$	volume of particle	[m <sup>3</sup> ]
$V_0$	volume of unit cell	[m <sup>3</sup> ]
$x_i$	particle size of fraction $i$	[m]
$Y$	Young's modulus of elasticity	[Pa]
$\delta$	solubility parameter	[Pa <sup>1/2</sup> ]
$\varepsilon$	porosity	[-]
$\ell$	flaw length	[m]
$\nu$	Poisson's ratio	[-]

## 2.9 References

1. Peukert W., 2002, Material properties in fine grinding. *10<sup>th</sup> European symposium on comminution*, Heidelberg, Germany.
2. Prasher C.L., 1987, *Crushing and grinding process handbook*.
3. Berthiaux H., Dodds J., 1996, Approximate calculation of breakage parameters from batch grinding tests. *Chem. Eng. Sci.* 51, 4509-4516.
4. Vogel L., Peukert W., 2002, Determination of material properties relevant to grinding by practicable lab scale milling tests. *10<sup>th</sup> European symposium on comminution*, Heidelberg, Germany.
5. Yashima S., Kanda Y., Sano S., 1987, Relationships between particle size and fracture energy or impact velocity required to fracture as estimated from single particle crushing. *Powder Technol.* 51, 277-282.
6. Griffith A.A., 1921, The phenomena of rupture and flow in solids. *Phil. Trans. R. Soc.* 221.
7. Weichert R., 1994, International Fine Particle research institute, Experimental Simulation of Processes in Ball Mills by Fragmentation of Particle Assemblies. International Fine Particle Research Institute FRR 05-10.
8. Potapov A.V., Campbell C.S., 2001, Parametric dependence of particle breakage mechanisms. *Powder Technol.* 120, 164-174.
9. Rumpf H., 1973, Physical aspects of comminution and a new formulation of a law of comminution. *Powder Technol.* 7, 145-159.
10. Marsh D.W., 1964, Plastic flow in glass. *Proc. Roy. Soc.* A279, 420-35.

11. Ghadiri M., Papadopoulos D.G., 1995, Impact Attrition of Particulate Solids. International Fine Particle Research Institute FRR 16-06.
12. Taylor L., Papadopoulos D., Mitchell J., Snowden M., 2004, Predicting bulk milling behaviour from single crystals. AAPS Annual Meeting and Exposition.
13. Schönert K., 1972, Role of fracture physics in understanding comminution phenomena. *Trans. AIME* 252, 21-26.
14. Vegt de O.M., Vromans H., Faassen F., Voort Maarschalk van der K., 2005, Milling of drug substance, part 2: Prediction of drug substance particle size distribution. *Part. Syst. Charact.* 22, 261-267
15. Hancock B.C., York P., Rowe R.C., 1997, The use of the solubility parameters in pharmaceutical dosage form design. *Int. J. Pharm.* 148, 1-21.
16. Hansen C.M., 1969, The universality of the solubility parameter. *Ind. Eng. Chem.* 8, 2-11.
17. Roberts R.J., Rowe R.C., York P., 1995, The relationship between the fracture properties, tensile strength and critical stress intensity factor of organic solids and their molecular structure. *Int. J. Pharm.* 125, 157-162.
18. Roberts R.J., Rowe R.C., York P., 1991, The relationship between Young's modulus of elasticity of organic solids and their molecular structure. *Powder Technol.* 65, 139-146.
19. Weibull W., 1951, A statistical distribution function of wide applicability. *J. Appl. Mechan.* 9, 293-297.
20. Heckel R.W., 1961B, Density-pressure relationships in powder compaction. *Trans. Met. Soc. AIME.* 221, 1001-1108
21. Roberts R.J., Rowe R.C., 1987, The compaction of pharmaceutical and other model materials - a pragmatic approach. *Chem. Eng. Sci.* 42, 903-911.
22. Szymanski A., Szymanski J., 1989, Hardness estimation of minerals rocks and ceramic materials. *Materials science monographs* 49, Elsevier, Amsterdam.

23. Tabor D., 1970, The hardness of solids. *Rev. Phys. Technology* 1, 145-179.
24. Nichols G., Frampton C.S., 1998, Physicochemical characterization of the orthorhombic polymorph of paracetamol crystallized from solution. *J. Pharm. Sci.* 87, 684-693.
25. Roberts R.J., Rowe R.C., 1994, The relationship between indentation hardness of organic solids and their molecular structure. *J. Mat. Science* 29, 2289-2296.
26. Roberts R.J., Rowe R.C., 1996, Influence of polymorphism on the Young's modulus and yield stress of carbamazepine, sulfathiazole and sulfanilamide. *Int. J. Pharm.* 129, 79-94.
27. Kopp S., Beyer C., Graf E., Kubel F., Doelker E., 1989, Methodology for a better evaluation of the relation between mechanical strength of solids and polymorphic form. *J. Pharm. Pharmacol.* 41, 79-82.
28. Doelker E., 1993, Comparative compaction properties of various microcrystalline cellulose types and generic products. *Drug Dev. Ind. Pharm.* 19, 2399-2471.
29. Roberts R.J., Rowe R.C., 1987, The Young's modulus of pharmaceutical materials. *Int. J. Pharm.* 37, 15-18.
30. Perry's Chemical Engineers' Handbook, 1997, 7<sup>th</sup> edition, McGraw-Hill

